

Supporting information for jp-2012-08461q:

**A Comparison of the Photoelectrochemical Behavior of H-Terminated and Methyl-Terminated Si(111) Surfaces in Contact with a Series of One-Electron, Outer-Sphere Redox Couples in CH<sub>3</sub>CN**

*Ronald L. Grimm, Matthew J. Bierman, Leslie E. O'Leary,  
Nicholas C. Strandwitz, Bruce S. Brunschwig, and Nathan S. Lewis\**

**Supporting Information**

*A. Calculation of the effective solution potential,  $E_{\text{eff}}(A/A^-)$  for comparisons of open-circuit photovoltages.*

Several previous reports established a linear relationship between the open-circuit photovoltage,  $V_{\text{oc}}$ , and solution redox potential,  $E(A/A^-)$ , for semiconductor liquid junctions,<sup>1-4</sup> but theoretical analysis demonstrates that this strict linearity only holds for certain types of changes the redox potential of the solution.<sup>5</sup> Specifically, changes to the concentration of the redox species that accepts the semiconductor majority carriers will effect a Nernstian shift in  $E(A/A^-)$ , but should not produce a change in  $V_{\text{oc}}$  for ideally-behaving systems. Thus, a rigorous evaluation of the relationship between  $V_{\text{oc}}$  and  $E(A/A^-)$  requires that this concentration dependence is consistently taken into account. Maintaining equal concentrations, or even comparable concentrations, of redox couples for different redox systems is challenging because it is not always possible to provide sufficient redox species to accept all of the light-limited photocarriers generated under 1 Sun illumination, especially for solubility-limited redox species, such as methyl viologen<sup>2+/•+</sup> in CH<sub>3</sub>CN.

The concentration corrections for the  $A/A^-$  redox species performed herein have followed conditions previously outlined.<sup>5</sup> Figure S1 highlights the effect of this concentration correction for an n-type semiconductor-liquid junction photoelectrochemical cell. Point **A** denotes an experimentally-obtained  $V_{\text{oc}}$  value at solution redox potential  $E(A/A^-)$  at which the concentrations of oxidized species

[A] and reduced species [A<sup>-</sup>] are not at ideal values for comparison to other photoelectrochemical  $V_{oc}$  vs  $E(A/A^-)$  values. To normalize to a consistent minority carrier acceptor concentration, we first consider the effect of changing the concentrations of the redox species from [A] and [A<sup>-</sup>], respectively, to [A]<sup>'</sup> and [A<sup>-</sup>]<sup>'</sup>, in a fashion such that [A]<sup>'</sup> =  $c[A]$  and [A<sup>-</sup>]<sup>'</sup> =  $c[A^-]$ . Such a uniform change in the redox species concentration ratio (i.e. dilution) does not change the Nernstian solution potential, but will effect a change on the  $V_{oc}$  for ideally-behaving systems over a certain range of the  $V_{oc}$  vs  $E(A/A^-)$  behavior. Equations S1 and S2 describe this change for n-type and for p-type semiconductor/liquid junctions, respectively.<sup>5</sup>

$$V'_{oc,n} = V_{oc,n} + \frac{k_B T}{q} \ln \frac{[A^-]}{[A^-]'} \quad (S1)$$

$$V'_{oc,p} = V_{oc,p} + \frac{k_B T}{q} \ln \frac{[A]}{[A]'} \quad (S2)$$

In eqs S1 and S2,  $k_B$  is Boltzmann's constant,  $T$  is the temperature, and  $q$  is the fundamental unit of charge. If [A<sup>-</sup>]<sup>'</sup> > [A<sup>-</sup>],  $V_{oc}$  would decrease from point **A** in Fig. S1 to point **B**, while  $E(A/A^-)$  remains unchanged. This open-circuit photovoltage,  $V_{oc}'$ , represents the value that would be obtained if the photoelectrochemical cell contained redox species in concentrations [A]<sup>'</sup> and [A<sup>-</sup>]<sup>'</sup>.

Rather than scaling an experimentally-acquired  $V_{oc}$  value, it is more instructive to scale the solution potential from  $E(A/A^-)$  to an effective value. From Fig. 3,  $V_{oc}$  scales directly with  $E(A/A^-)$  for n-type semiconductors. For p-type semiconductors,  $V_{oc}$  scales in the same fashion, with a negative sign, with respect to changes in  $E(A/A^-)$ . Thus eqs S3 and S4 describe the linear change in  $V_{oc}$  between two electrochemical cells with redox couples  $A/A^-$  and  $B/B^-$  when [A] = [B] and [A<sup>-</sup>] = [B<sup>-</sup>]. Equations S3 and S4 describe the change for n-type and p-type semiconductor/liquid junctions, respectively.

$$V_{oc,n,b} = V_{oc,n,a} + E(B/B^-) - E(A/A^-) \quad (S3)$$

$$V_{oc,p,b} = V_{oc,p,a} - E(B/B^-) + E(A/A^-) \quad (S4)$$

The shift from point **B** to point **C** in Fig. S1 represents the change in  $V_{oc}$  at an n-type semiconductor accompanied by a shift in solution potential from  $E(A/A^-)$  to  $E(B/B^-)$  when  $[A]^+ = [B]$  and when  $[A]^+ = [B]$  and when  $[A^-] = [B^-]$ . Thus, the overall shift from point **A** to point **C** represents the shift to the effective solution potential,  $E_{eff}(A/A^-)$ , that is needed for the comparison of  $V_{oc}$  vs  $E(A/A^-)$  relationships that have been determined by measurement using different redox species at mutually different solution concentrations. For n-type semiconductors in contact with redox couple  $A/A^-$ , the shift from  $E(A/A^-)$  to  $E_{eff}(A/A^-)$  follows eq S5, which combines S1 and S3.

$$E_{eff}(A/A^-) = E(A/A^-) + \frac{k_B T}{q} \ln \frac{[A^-]}{[A^-]_{eff}} \quad (S5)$$

Similarly, eq S6 combines eqs S2 and S4 to describe the corresponding shift from  $E(A/A^-)$  to  $E_{eff}(A/A^-)$  for p-type semiconductors.

$$E_{eff}(A/A^-) = E(A/A^-) - \frac{k_B T}{q} \ln \frac{[A^-]_{eff}}{[A^-]} \quad (S6)$$

For the experimental data, Table 1 in the manuscript reports values of  $E_{eff}(A/A^-)$  vs SCE for comparison with previous results, in which the minority carrier acceptor concentrations are normalized to 10 mM.

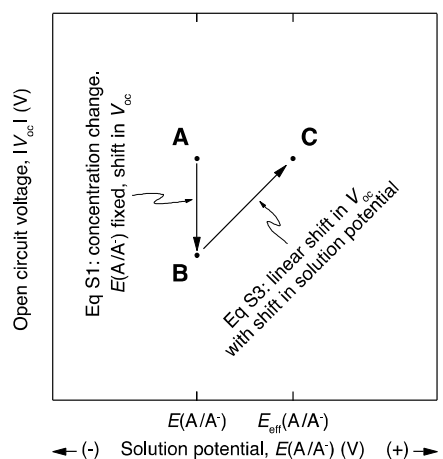


Figure S1. Graphical representation of the shift in experimental solution potential  $E(A/A^-)$  to an effective potential  $E_{eff}(A/A^-)$  for comparison of  $V_{oc}$  vs  $E(A/A^-)$ .

### *B. X-ray photoelectron spectroscopic surface characterization.*

A Surface Science Instruments M-Probe system was used to acquire the XPS spectra of the O 1s, C 1s, and Si 2p regions. Data were acquired using the ESCA25 Capture (Service Physics, Bend OR; V5.01.04) software. Samples were introduced through a fast-entry load lock to an ultra high vacuum analysis chamber that had a base pressure  $< 2 \times 10^{-9}$  Torr. A monochromatic x-ray source illuminated the sample with 1486.6 eV Al K $\alpha$  radiation that was directed at 35° to the sample surface. A 100 mm radius hemispherical energy analyzer, with a pass energy of 50 eV collected photoelectrons. The analyzer had a resolution of  $\sim 0.8$  eV and a takeoff angle of 35° with respect to the sample surface. A low-resolution survey scan verified the absence of other contaminants on the electrode surface. Data were evaluated using a custom LabVIEW-based software package.

For the methylated Si(111) samples, XPS was used to quantify the degree of surface oxidation and to evaluate the effectiveness of methylation against deleterious surface oxidation.<sup>6</sup> Figure S2 presents a representative spectrum of a methylated Si(111) wafer that had been exposed to air ambient for 8 days prior to XPS analysis. The black circles denote the acquired data following the subtraction of a Shirley-type baseline (red trace). The solid blue traces and dashed blue sum correspond to a fit to the feature at  $\sim 99$  eV that can be ascribed to photoelectron emission from neutral Si. These traces correspond to a Si 2p<sub>3/2</sub> peak centered at 99.09 eV and a Si 2p<sub>1/2</sub> peak at 99.76 eV. Photoelectrons from oxidized silicon samples typically exhibit a feature at  $\sim 103$  eV, a region magnified 10-fold in the inset. While no distinct feature exists in this region, the green trace denotes a simulated peak corresponding to  $\sim 1$  % of the area under the blue traces.

In accord with previous reports, comparison of the peak areas in Fig. S2 indicates that the methyl termination effectively passivated the silicon surfaces against oxidation. Based on the photoelectron energy, overlayer thickness, and instrument sensitivity factors, a completely oxidized silicon monolayer

on Si(111) would yield an area ratio of the oxidized Si 2p photoelectron feature at 103 eV to the neutral Si 2p feature at 99 eV of  $\sim 0.21$ .<sup>7</sup> Because the 1 % area ratio of the green trace to the blue trace overestimates the oxidation, the XPS results indicate that the degree of silicon surface oxidation is less than 5 % of a monolayer, and is bounded by the sensitivity limits of the instrument.

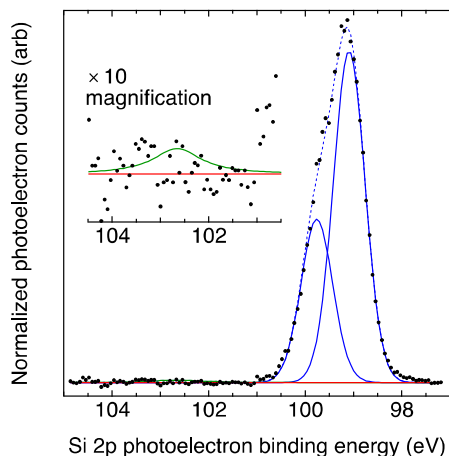


Figure S2. XP spectrum of the Si 2p region of a silicon wafer following methylation and exposure to air ambient for 8 days. While the black dots indicate the acquired data, the blue traces denote fitted peaks attributed to non-oxidized Si 2p<sub>3/2</sub> and 2p<sub>1/2</sub> photoelectrons at 99.09 eV and 99.76 eV, respectively. Although no significant signal appears at 103 eV indicative of photoelectrons from oxidized silicon, the green trace presents a simulated peak corresponding to 1% of the area under the blue curves. The green trace poorly fits the photoelectron data indicating a low degree of oxidation in the silicon sample. The red trace denotes a Shirley-type baseline that was previously subtracted from all curves and data.

### Supporting Information References

- (1) Heller, A.; Lewerenz, H. J.; Miller, B. *J. Am. Chem. Soc.* **1981**, *103*, 200.
- (2) Heller, A.; Miller, B.; Thiel, F. A. *Appl. Phys. Lett.* **1981**, *38*, 282.
- (3) Lewis, N. S. *J. Electrochem. Soc.* **1984**, *131*, 2496.
- (4) Rosenbluth, M. L.; Lewis, N. S. *J. Am. Chem. Soc.* **1986**, *108*, 4689.
- (5) Rosenbluth, M. L.; Lewis, N. S. *J. Phys. Chem.* **1989**, *93*, 3735.
- (6) Bansal, A.; Li, X. L.; Lauermann, I.; Lewis, N. S.; Yi, S. I.; Weinberg, W. H. *J. Am. Chem. Soc.* **1996**, *118*, 7225.
- (7) Haber, J. A.; Lewis, N. S. *J. Phys. Chem. B* **2002**, *106*, 3639.